

Modulated Structures for Incommensurate Monolayer Solid Phases of D₂ Physisorbed on Graphite

Jinhe Cui and Samuel C. Fain, Jr.

Department of Physics, University of Washington, Seattle, Washington 98195

H. Freimuth and H. Wiechert

Institut für Physik, Johannes Gutenberg-Universität, D-6500 Mainz, Federal Republic of Germany

and

H. P. Schildberg and H. J. Lauter

Institut Laue-Langevin, 38042 Grenoble-Cedex, France

(Received 22 October 1987)

Neutron and low-energy electron diffraction at $2\text{ K} \leq T \leq 5\text{ K}$ are used to determine the structure of three incommensurate (IC) solid phases for D₂ on graphite. The α phase is a uniaxial IC solid phase with striped domain walls due to strong substrate-induced modulation of the nearest-neighbor spacing. The γ phase is a rotated triangular IC phase with satellite diffraction peaks due to modulation intermediate between that of the α phase and the Novaco-McTague rotated IC phase which exists at higher density.

PACS numbers: 68.35.Rh, 61.12.Gz, 61.14.Hg, 67.70.+n

The modulation of the nearest-neighbor distance of an incommensurate (IC) monolayer by periodic adsorbate-substrate forces leads to several types of IC phases which are theoretically understood and experimentally observed. For spherical molecules on a triangular substrate in the weak-modulation limit, the lower energy of transverse modulations compared to longitudinal modulations can produce a Novaco-McTague (NM) effect in which the monolayer is rotated away from substrate high-symmetry directions.^{1,2} In the intermediate-modulation limit, there can be a continuous transition between nonrotated and rotated triangular monolayer phases as the number of molecules on the substrate is varied.²⁻⁵ In the strong-modulation limit, a uniaxial IC (UIC) domain-wall phase with completely different symmetry can occur.^{4,6}

We show here that the system D₂ on graphite has a UIC phase with striped domain walls of width less than 10 Å for wall spacings between 20 and 40 Å at $T \leq 6\text{ K}$. These walls are sharper than the widths deduced for Kr and Xe on graphite^{3,5} or Xe on Pt(111).⁴ In addition to the UIC phase, the D₂ monolayer on graphite has a novel intermediate phase at $T \leq 10\text{ K}$ (called the γ phase^{7,8}) which is a rotated and modulated triangular phase with rotation angle *greater than* that of the higher-density rotated IC (RIC) phase. Such an intermediate phase has not been theoretically predicted and is quite different from the nonrotated triangular IC phase seen in other systems.³⁻⁵ The RIC phase is rotated at $T = 5\text{ K}$ approximately as predicted by the NM continuum theory.¹

The commensurate $(\sqrt{3} \times \sqrt{3})R30^\circ$ (C) phase of the D₂ monolayer has been experimentally investigated by neutron diffraction,⁹ nuclear magnetic resonance,¹⁰ and

heat capacity.⁷ Until recently, the main information available about higher-density phases was that a triangular IC phase was formed for *o*-D₂ at higher coverages.⁹ Recent heat-capacity measurements for IC densities have indicated several intermediate phases,^{7,8} which motivated the present diffraction measurements. The fact that the γ phase occurs for D₂ and not for the isotopes HD and H₂ (Ref. 7) which have larger zero-point motion¹¹ suggests that the γ phase is due to the less pronounced quantum aspects of D₂.

LEED measurements on normal D₂ gas¹² were performed in Seattle. A Kish graphite crystal and crystals extracted from calcite gave identical results within experimental resolution. Room-temperature gas was admitted via a tube ending about 3 cm from the graphite sample to minimize contamination due to impurity gases. Diffraction patterns were observed with 62.5-eV electrons incident within 3° of the surface normal. The electron beam was turned on only for 0.5 sec for each observation to minimize electron-induced desorption effects. The coverage of the monolayer was changed by variation of the gas flux. The monolayer density ρ (normalized to 1.00 for the ideal C density) was determined from the diffraction pattern of the IC layer. The LEED diffraction profiles in γ and IC phases were limited by instrumental resolution and substrate perfection to 0.04 Å⁻¹ (FWHM).

Neutron-diffraction measurements were performed in Grenoble. Two forms of exfoliated graphite substrate were used: Papyex and ZYX.¹³ Peak positions and relative intensities were identical within experimental errors for the two substrates; some of the ZYX data are discussed in more detail elsewhere.⁴ The coverage n used here is proportional to the amount of gas adsorbed on the

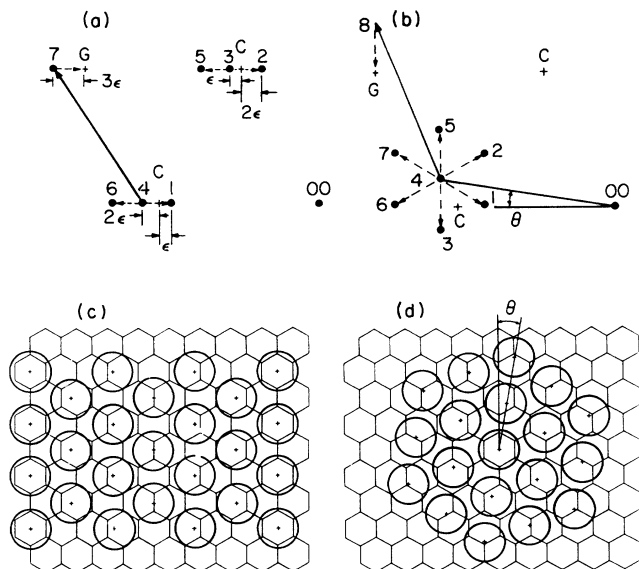


FIG. 1. Reciprocal- and real-space diagrams for UIC and γ solid phases. In (a) and (b) the specular peak is denoted by 00; the first-order commensurate peaks by C; first-order graphite peaks by G. Numbered peaks are discussed in text. (a) Uniaxial IC (α) structure at $\rho=1.126$. Some peak displacements from C positions are given in multiples of ϵ . (b) D_2 γ structure at $\rho=1.25$ considered as a triangular IC structure rotated by θ from the C direction. (c) Unmodulated real-space structure of the UIC phase at $\rho=1.126$. Graphite-induced modulation occurs along the horizontal direction. (d) Unmodulated real-space structure of the γ phase at $\rho=1.25$.

exfoliated graphite, with the proportionality constant determined from the amount of gas required to produce an IC monolayer having a known density.^{14,15}

In the LEED measurements the diffraction peaks at 5 K became broader when the gas flux was increased above the minimum necessary to produce the C pattern. When the broad peaks could be resolved into component peaks, the LEED pattern consisted of peaks 1-4 of Fig. 1(a) from three UIC domains rotated 120° apart. These peaks shifted continuously from the C position with increasing flux. At the beginning of some experiments on the Kish graphite, one UIC domain direction was more intense than the other two, because of an anisotropic nucleation process. This is a clear evidence that the α phase⁸ is a UIC structure.

Single scattering from an unmodulated UIC structure [Fig. 1(c)] would produce only peaks 3, 4, and 7 for the region of reciprocal space shown in Fig. 1(a)⁶; these peaks are displaced from the C peaks by ϵ , 2ϵ , and 3ϵ . Because theory predicts that the UIC phase exists as a result of domain-wall energetics,⁶ a modulated structure is expected.^{16,17} The wave vector of the modulation is given by dashed vectors, such as the one from peak 7 to G, which are added to peaks 3 and 4, giving peaks 1, 2, 5, and 6. Figure 2 compares the predicted positions

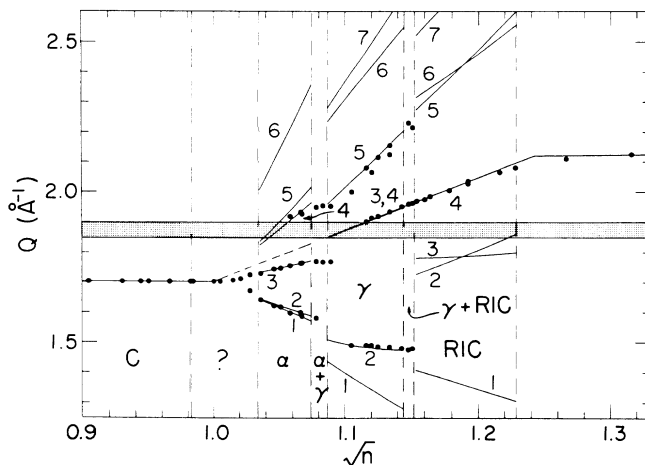


FIG. 2. Neutron-diffraction peak position (Q) vs square root of coverage (\sqrt{n}) for D_2 at $2 \text{ K} \leq T \leq 4 \text{ K}$. The solid lines in the α , γ , and RIC phases are positions predicted for the peaks shown in Figs. 1(a) and 1(b). The dashed line in the α region is that expected if this were a triangular structure. For this graph the coverage n is normalized to the density calculated from Q at one coverage in the IC density range (Refs. 14 and 15). The vertical lines with phase identifications between them are from LEED measurements at 5 K, except for the vertical line at $\sqrt{n}=0.983$ which indicates the coverage n at which the C phase heat-capacity peak is maximum ($n=1$ in Refs. 7 and 8). The $\alpha+\gamma$ coexistence region shown is consistent with the neutron and heat-capacity measurements.

(solid lines) with the observed positions of the neutron peaks at $2 \leq T \leq 4 \text{ K}$.^{8,14,15} Interference from the 002 reflections from misoriented graphite crystallites prevents accurate measurements for the shaded range of reciprocal-space vectors Q between 1.85 and 1.90 \AA^{-1} . The data are plotted as Q vs \sqrt{n} to facilitate comparison with data at higher densities.⁹ (The main peak would follow the dashed line if the α phase were a triangular structure.) The correct coverage dependence of the peak positions in the α phase is additional evidence that the α phase is a UIC structure.

For a UIC phase, the amount of the modulation can be estimated for rigid walls if a domain-wall profile is assumed.¹⁷ With use of the domain-wall profile of Gordon and Lançon,¹⁸ the domain-wall width was determined by comparison of calculated intensities to observed neutron intensities for peaks 1 + 2 and 3. The ratio of the satellite intensity (1 + 2) to the main peak (3) for D_2 on Papyex^{8,15} and ZYX graphite¹⁴ varied from 0.25 ± 0.02 at $n=1.06$ to 0.08 ± 0.01 at $n=1.14$, consistent with an effective domain-wall width of about 10 \AA . Over this range in n , the average wall spacing varies from 20 to 40 \AA , indicating that the domain-wall limit is realized throughout the α phase.

As the number of molecules on the surface was increased above $n=1.14$, a first-order transition was observed to a new phase with different diffraction peaks,

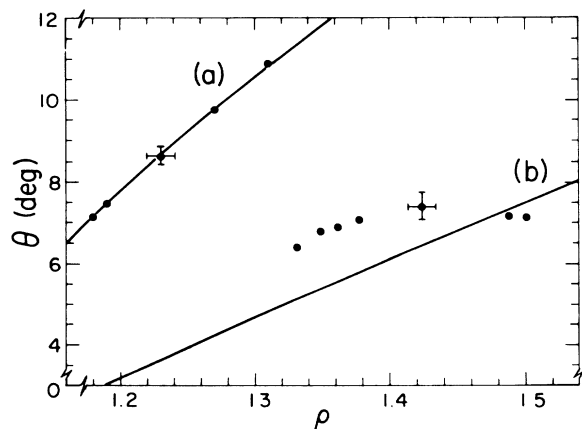


FIG. 3. Rotation angle (θ) vs monolayer density (ρ) determined from LEED measurements for the γ and RIC phases of D_2 near 5 K. The upper curve (a) is determined by the requirement that the modulation wave vector of the γ phase is along the graphite symmetry direction as in Fig. 1(b); the lower curve (b) is the NM result (Ref. 1) with the central-force sound-velocity ratio. Error bars show typical measurement uncertainties.

the γ phase.⁸ The LEED pattern of the γ phase consisted of peaks 1, 3, and 4 in Fig. 1(b).¹⁶ The γ phase can be described as a rotated triangular phase [Fig. 1(d)] with modulation due to the substrate. The modulation wave vector is indicated by the arrow pointing from 8 to G^1 ; the orientation of the LEED diffraction pattern is such that this vector is always along one of the graphite six-fold symmetry directions to within 0.4° for the γ phase. This orientation leads to the curve of rotation angle θ versus monolayer density ρ , curve a in Fig. 3, and causes the LEED peaks 1, 3, and 4 for the $+\theta$ domain to coincide with peaks 1, 4, and 3 for the $-\theta$ domain.

In a first-order approximation, the positions of modulation satellites^{1,17} are obtained by addition of a star of six wave vectors like that from 8 to G in Fig. 1(b) to the mean lattice peak 4. The predicted satellite positions of peaks 1-3 and 5-7 in Fig. 1(b) are plotted by solid lines in Fig. 2 for the γ phase. Two of these modulation satellites (2 and 5) were clearly observed by neutrons. The ratio of the satellite intensity (2 or 5) to the main peak (3+4) was 0.5 ± 0.01 for $1.25 < n < 1.32$. The absence of any significant change in intensity ratio with density is quite different than for the α phase.

The special rotation angle of the γ phase produces LEED and neutron-diffraction peaks at the same positions as for a hexagonal heavy-wall structure¹⁷; this implies that the lateral modulation can also be described by such a domain-wall structure. In the sharp domain-wall limit, the peaks 1, 3, and 4 in Fig. 1(b) have equal intensity for a hexagonal heavy-wall phase.¹⁷ The fact that peaks 2 and 5 are the largest-intensity satellites, with an approximately constant intensity relative to the main peak, indicates that the domain walls in the γ phase are

broad and overlapping. Thus it is more useful to think of the γ phase as a modulated triangular phase than as a domain-wall phase.

As the number of molecules was increased above $n=1.32$, the γ phase was observed to coexist with a higher-density RIC phase. One major difference between the γ phase and the RIC phase is that the values of θ vs ρ deduced from LEED for the RIC phase at 5 K (filled circles in Fig. 3) lie close to those predicted by the NM result with the central-force sound-velocity ratio¹ shown by curve b. (LEED data for the RIC phases of H_2 and HD, where no γ phase has been found for $T > 2$ K, also lie close to curve b.¹⁹)

In neutron diffraction the major difference between the γ and RIC phases is the absence of any detectable satellites for the RIC phase. In Fig. 2 the expected satellite positions are plotted (solid lines) from the rotation angle measured by LEED with a construction similar to Fig. 1(b).^{1,17} (However, the direction of the modulation wave vector changes with density for the RIC phase as expected from Ref. 1.) The apparent absence of neutron-diffraction satellites in the RIC phase indicates a smaller density modulation in this phase than for the α and the γ phases. This is consistent with the fact that the rotation angles of the RIC phase approximately follow the prediction of the NM model which assumes a weak substrate modulation.

In the RIC phase separate LEED peaks are observed for the $+\theta$ and $-\theta$ rotated domains. The presence of LEED peaks analogous to 1 and 3 for the γ phase in the weakly modulated RIC phase indicates significant double scattering at the LEED energy used.¹⁶ As the change in the relative peak intensities in LEED at the γ -RIC transition is small, the LEED peak 1 in the γ phase is also due to double scattering.

In summary, we have shown that D_2 on graphite provides a system which goes from the domain-wall limit (α phase) to the weakly modulated limit (RIC phase) via an intermediate-modulated solid (γ) phase of heavy-wall symmetry. The α phase is shown to be a UIC phase with striped domain walls of width less than 10 \AA for wall spacings between 20 and 40 \AA . The γ phase is the first example where the modulation satellites are observed for a rotated triangular monolayer phase. The detailed neutron measurements of the satellite intensity cited above provide important data for the theoretical modeling of an oriented monolayer film beyond the weak substrate-modulation limit. The RIC phase is oriented approximately as predicted by NM theory.¹ The C- α transition region is discussed elsewhere.¹⁴

Professor H. Suematsu kindly supplied Kish graphite single crystals used for some of the LEED measurements. R. Birgeneau, L. Bruch, M. Den Nijs, M. Kardar, A. Novaco, L. Sorensen, and O. Vilches provided helpful comments. The LEED work was supported by the National Science Foundation Low Temperature

Physics Program (U.S.A.) under Grant No. DMR 85-13191. The neutron work was partially funded by the German Federal Minister of Research and Technology (BMFT) under Contract No. 05 353 AA I2.

¹J. P. McTague and A. D. Novaco, Phys. Rev. B **19**, 5299 (1979).

²H. Shiba, J. Phys. Soc. Jpn. **48**, 211 (1980), and **46**, 1852 (1979).

³E. D. Specht, A. Mak, C. Peters, M. Sutton, R. J. Birgeneau, K. L. d'Amico, D. E. Moncton, S. E. Nagler, and P. M. Horn, Z. Phys. B **69**, 347 (1987).

⁴K. Kern, Phys. Rev. B **35**, 8265 (1987).

⁵H. Hong, C. J. Peters, A. Mak, R. J. Birgeneau, P. M. Horn, and H. Suematsu, Phys. Rev. B **36**, 7311 (1987).

⁶P. Bak, D. Mikamel, J. Villain, and K. Wentowska, Phys. Rev. B **19**, 1610 (1979).

⁷H. Freimuth and H. Wiechert, Surf. Sci. **178**, 716 (1986).

⁸H. Wiechert, H. Freimuth, H. P. Schildberg, and H. J. Lauter, Jpn. J. Appl. Phys. **26**, Suppl. 26-3, 351 (1987).

⁹M. Nielsen, J. P. McTague, and L. Passell, in *Phase Transitions in Surface Films*, edited by J. G. Dash and J. Ruvalds (Plenum, New York, 1980), p. 127.

¹⁰P. R. Kubik, W. N. Hardy, and H. Glattli, Can. J. Phys.

63, 605 (1985).

¹¹X.-Z. Ni and L. W. Bruch, Phys. Rev. B **33**, 4584 (1986).

¹²The presence of 33% *p*-D₂ molecules in normal D₂ is not expected to affect the results since molecular-axis orientational ordering has not been detected down to 0.3 K (Ref. 10).

¹³Papyex is a trademark of Carbon Lorraine; ZYX is a trademark of Union Carbide.

¹⁴H. P. Schildberg, H. J. Lauter, H. Freimuth, H. Wiechert, and R. Haensel, Jpn. J. Appl. Phys. **26**, Suppl. 26-3, 345 (1987).

¹⁵H. J. Lauter, H. P. Schildberg, H. Godfrin, H. Wiechert, and R. Haensel, Can. J. Phys. **65**, 1435 (1987).

¹⁶In LEED measurements peaks 1 and 2 in Fig. 1(a) and 1 and 3 in Fig. 1(b) can occur even for unmodulated structures as a result of double diffraction involving one substrate vector **G** and one first-order overlayer diffraction vector of the unmodulated structure [3 and 4 in Fig. 1(a) or 4 in Fig. 1(b)]. Peaks 7 in Fig. 1(a) and 8 in Fig. 1(b) are outside the acceptance angle of the LEED detector for the experimental conditions used.

¹⁷M. Nielsen, J. Als-Nielsen, and J. P. McTague, in *Ordering in Two Dimensions*, edited by S. Sinha (Elsevier North-Holland, New York, 1980), p. 135. The hexagonal domain structure with $\Delta a/a = \frac{1}{3}$ is identical with a hexagonal heavy-wall structure.

¹⁸M. B. Gordon and F. Lançon, J. Phys. C **18**, 3929 (1985).

¹⁹J. Cui and S. C. Fain, Jr., unpublished.

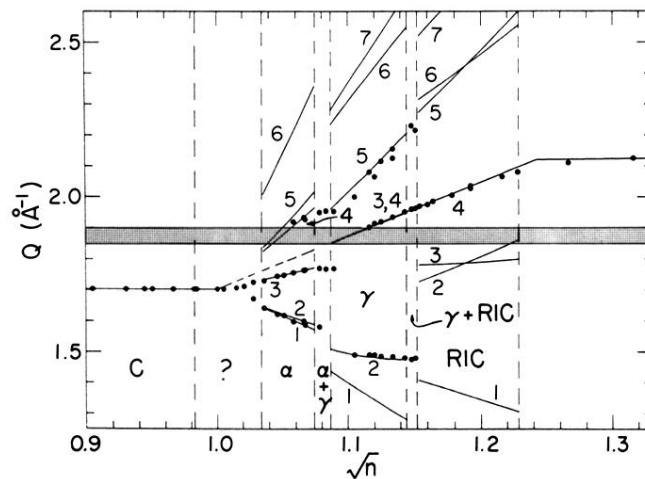


FIG. 2. Neutron-diffraction peak position (Q) vs square root of coverage (\sqrt{n}) for D_2 at $2 \text{ K} \leq T \leq 4 \text{ K}$. The solid lines in the α , γ , and RIC phases are positions predicted for the peaks shown in Figs. 1(a) and 1(b). The dashed line in the α region is that expected if this were a triangular structure. For this graph the coverage n is normalized to the density calculated from Q at one coverage in the IC density range (Refs. 14 and 15). The vertical lines with phase identifications between them are from LEED measurements at 5 K, except for the vertical line at $\sqrt{n} = 0.983$ which indicates the coverage n at which the C phase heat-capacity peak is maximum ($n = 1$ in Refs. 7 and 8). The $\alpha + \gamma$ coexistence region shown is consistent with the neutron and heat-capacity measurements.